

Translocation Dynamics with Attractive Nanopore-Polymer Interactions

Kaifu Luo,^{1,*} Tapio Ala-Nissila,^{1,2} See-Chen Ying,² and Aniket Bhattacharya³

¹*Department of Engineering Physics, Helsinki University of Technology,
P.O. Box 1100, FIN-02015 TKK, Espoo, Finland*

²*Department of Physics, Box 1843, Brown University, Providence, Rhode Island 02912-1843, USA*

³*Department of Physics, University of Central Florida, Orlando, Florida 32816-2385, USA*

(Dated: November 2, 2018)

Using Langevin dynamics simulations, we investigate the influence of polymer-pore interactions on the dynamics of biopolymer translocation through nanopores. We find that an attractive interaction can significantly change the translocation dynamics. This can be understood by examining the three components of the total translocation time $\tau \approx \tau_1 + \tau_2 + \tau_3$ corresponding to the initial filling of the pore, transfer of polymer from the *cis* side to the *trans* side, and emptying of the pore, respectively. We find that the dynamics for the last process of emptying of the pore changes from non-activated to activated in nature as the strength of the attractive interaction increases, and τ_3 becomes the dominant contribution to the total translocation time for strong attraction. This leads to a new dependence of τ as a function of driving force and chain length. Our results are in good agreement with recent experimental findings, and provide a possible explanation for the different scaling behavior observed in solid state nanopores *vs.* that for the natural α -hemolysin channel.

PACS numbers: 87.15.A-, 87.15.H-

I. INTRODUCTION

The controlled transport of polymer molecules through a nanopore has received increasing attention due to its importance in biological systems and its potentially revolutionary technological applications [1, 2]. There is a flurry of experimental [3, 4, 5, 6, 7, 8, 9, 10, 11, 12, 13, 14, 15, 16, 17, 18, 19, 20, 21] and theoretical [21, 22, 23, 24, 25, 26, 27, 28, 29, 30, 31, 32, 33, 34, 35, 36, 37, 38, 39, 40, 41, 42, 43, 44, 45, 46, 47, 48, 49, 50, 51, 52, 53, 54, 55, 56, 57, 58, 59, 60, 61, 62, 63, 64, 65, 66] studies devoted to this subject. In an important experiment, Kasianowicz *et al.* [1] demonstrated that an electric field can drive single-stranded DNA and RNA molecules through the water-filled α -hemolysin channel and that the passage of each molecule is signaled by a blockade in the channel current. These observations can be used to directly characterize the polymer length. Similar experiments have been done recently using solid state nanopores with more precisely controlled dimensions [12, 13, 14, 15, 16, 17, 18, 19, 20, 21]. Currently, extensive effort is being taken to unravel the dependence of the translocation time τ on the system parameters such as the polymer chain length N [5, 6, 21, 23, 26, 27, 29, 32, 38, 39, 40, 41, 42, 43, 44, 45, 46, 47, 48, 49, 50, 60], pore length L and pore width W [45], driving force F [5, 6, 9, 11, 32, 39, 46, 47, 60], sequence and secondary structure [3, 4, 6, 49, 50], and polymer-pore interactions [4, 6, 29, 50, 51, 52, 60, 63].

Meller *et al.* [4, 6] have shown how several different DNA polymers can be identified by a unique pat-

tern in an “event diagram”. The event diagrams are plots of translocation duration versus blockade current for an ensemble of events. Patterns for a given polymer can be characterized uniquely by the blockade current, the translocation time and its distribution. Because each type of polynucleotide gives rise to specific values of these three parameters, DNA molecules which differ from each other only by sequence can be distinguished. At room temperature striking differences were found for the translocation time distributions of polydeoxyadenylic acid (poly(dA)₁₀₀) and polydeoxycytidylic acid (poly(dC)₁₀₀) DNA molecules. The translocation time of poly(dA) is found to be much longer, and its distribution is wider with a longer tail compared with the corresponding data for poly(dC). Moreover, the differences between the translocation behavior are accentuated at lower temperature. The origin of the different behavior was attributed to stronger attractive interaction of poly(dA) with the pore. Recently Krasilnikov *et al.* [67] have investigated the dynamics of single neutral poly(ethylene glycol) (PEG) molecules in the α -hemolysin channel in the limit of a strong attractive polymer-pore attraction. The result for the residence time in the channel shows a novel non-monotonic behavior as a function of the molecular weight. The other experimental data that point to the possible essential role of the monomer-pore interaction concerns the different conflicting values of scaling exponents of τ with N and with the applied voltage as reported in recent experiments. A linear dependence $\tau \sim N$ was observed for polymer translocation through α -hemolysin channel [1, 5], while another experiment reported that $\tau \sim N^{1.27} \approx N^{2\nu}$ for a synthetic nanopore [21], where ν is the Flory exponent [68, 69]. As to the dependence of the translocation time on the applied voltage for α -hemolysin channel, an inverse linear behavior [1] is observed for polyuridylic

*Author to whom the correspondence should be addressed; Electronic address: luokaifu@gmail.com

acid (poly(U)) while an inverse quadratic dependence [5] is found for polydeoxyadenylic acid (poly(dA)). One possible explanation for all these conflicting data is that the polymer-pore interaction depends crucially on the details of the pore structure (α -hemolysin channel vs synthetic nanopore) in addition to being base pair specific.

To date, most of the theoretical studies of the translocation of biopolymers through nanopore are based on models in which the wall of the pore only plays a passive role in confining the polymer to the inside of the pore. There are only a few theoretical studies of such interaction effects. Based on a Smoluchowski equation with a phenomenological microscopic potential to describe the polymer-pore interactions, Lubensky and Nelson [29] captured the main ingredients of the translocation process. However, when comparing with experiments, their model is not sufficient. Numerically, Tian and Smith [60] found that attraction facilitates the translocation process by shortening the translocation time, which contradicts experimental findings [4, 6]. In a recent letter [50], we used Langevin dynamics (LD) simulations to investigate the influence of polymer-pore interactions on translocation. We found that with increasing attraction, the histogram for the translocation time τ shows a transition from Gaussian distribution to a long-tailed distribution corresponding to thermal activation over a free energy barrier. The N dependence of the entropic force leads to both the translocation time and the residence time in the pore showing a non-monotonic behavior as a function of N for short chains in the strong attraction limit. These results are in good agreement with the above experimental data [4, 6, 67].

In the present work, we further show that strong polymer-pore interactions can directly affect the *effective* scaling exponents of τ both with N and with the applied voltage, which provides a possible explanation for the different experimental findings [1, 5, 21] on these physical quantities. We provide a microscopic understanding of how strong polymer-pore interaction influences the translocation dynamics. This is done through analyzing the three quantities τ_1 , τ_2 and τ_3 corresponding to initial filling of the pore, transfer of the polymer from the *cis* side to the *trans* side, and finally emptying of the pore, respectively. We find that the final process of emptying the pore τ_3 involves an activation barrier and completely dominates the translocation time in the strong attractive interaction limit. This leads to a strong dependence of the *effective* scaling exponents associated with the translocation time *both* on the strength of the attraction *and* the driving force. In addition, we examine the waiting time and residence time distributions. These quantities are related to the translocation time but the waiting time provides more detailed information about the translocation dynamics, while the residence time is the more relevant quantity for direct comparison with the experimental observation.

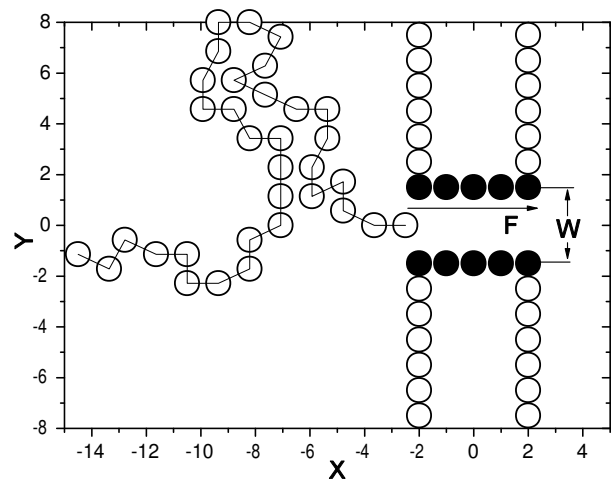


FIG. 1: A schematic representation of the system. The pore length $L = 5$ and the pore width $W = 3$ (see text for the units).

II. MODEL AND METHODS

In our numerical simulations, the polymer chains are modeled as bead-spring chains of Lennard-Jones (LJ) particles with the Finite Extension Nonlinear Elastic (FENE) potential. Excluded volume interaction between monomers is modeled by a short range repulsive LJ potential: $U_{LJ}(r) = 4\epsilon[(\frac{\sigma}{r})^{12} - (\frac{\sigma}{r})^6] + \epsilon$ for $r \leq 2^{1/6}\sigma$ and 0 for $r > 2^{1/6}\sigma$. Here, σ is the diameter of a monomer, and ϵ is the depth of the potential. The connectivity between neighboring monomers is modeled as a FENE spring with $U_{FENE}(r) = -\frac{1}{2}kR_0^2 \ln(1 - r^2/R_0^2)$, where r is the distance between consecutive monomers, k is the spring constant and R_0 is the maximum allowed separation between connected monomers.

We consider a 2D geometry as shown in Fig. 1, where the wall in the y direction is described as stationary particles within a distance σ from each other. The pore of length L and width W in the center of the wall is composed of stationary black particles. Between all monomer-wall particle pairs, there exist the same short range repulsive LJ interaction as described above. The pore-monomer interaction is modeled by a LJ potential with a cutoff of 2.5σ and interaction strength ϵ_{pm} . This interaction can be either attractive or repulsive depending on the position of the monomer from the pore particles. In the Langevin dynamics simulation, each monomer is subjected to conservative, frictional, and random forces, respectively, with [70] $m\dot{\mathbf{r}}_i = -\nabla(U_{LJ} + U_{FENE}) + \mathbf{F}_{\text{ext}} - \xi\mathbf{v}_i + \mathbf{F}_i^R$, where m is the monomer's mass, ξ is the friction coefficient, \mathbf{v}_i is the monomer's velocity, and \mathbf{F}_i^R is the random force which satisfies the fluctuation-dissipation theorem. The external force is expressed as $\mathbf{F}_{\text{ext}} = F\hat{x}$, where F is the external force strength exerted on the monomers in the pore, and \hat{x} is a unit vector in the direction along the pore axis.

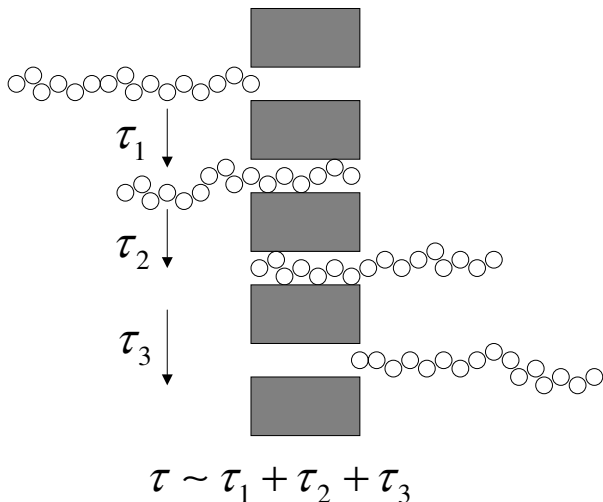


FIG. 2: Three components of the translocation process.

In the present work, we use the LJ parameters ε and σ and the monomer mass m to fix the energy, length and mass scales respectively. Time scale is then given by $t_{LJ} = (m\sigma^2/\varepsilon)^{1/2}$. The dimensionless parameters in our simulations are $R_0 = 2$, $k = 7$, $\xi = 0.7$ and $k_B T = 1.2$ unless otherwise stated. For the pore, we set $L = 5$ unless otherwise stated. A choice of $W = 3$ ensures that the polymer encounters an attractive force inside the pore. The driving force F is set between 0.5 and 2.0, which correspond to the range of voltages used in the experiments [1, 5]. The Langevin equation is integrated in time by a method described by Ermak and Buckholz [71] in 2D. Initially, the first monomer of the chain is placed in the entrance of the pore, while the remaining monomers are under thermal collisions described by the Langevin thermostat to obtain an equilibrium configuration. Typically, we average our data over 2000 independent runs.

III. RESULTS AND DISCUSSION

A. Translocation time, waiting time and residence time

The translocation time is defined as the time interval between the entrance of the first segment into the pore and the exit of the last segment. We can break down the translocation process into three components, as shown in Fig. 2. The total translocation time τ can be written as a sum of three contributions $\tau \approx \tau_1 + \tau_2 + \tau_3$, where τ_1 , τ_2 and τ_3 correspond to initial filling of the pore, transfer of the polymer from the *cis* side to the *trans* side, and finally emptying of the pore, respectively. To shed light on the detailed translocation process, we examine the number of translocated monomers n_{trans} as a function of the time for a typical successful translocation event for $N = 128$, and two values of the monomer attractive interaction

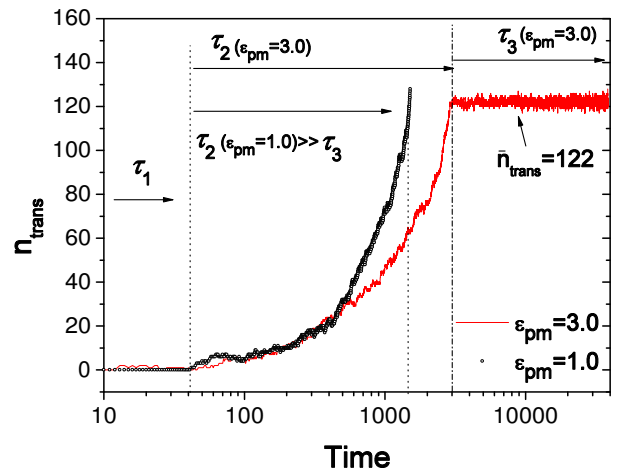


FIG. 3: Number of translocated monomers n_{trans} as a function of the time for $\varepsilon_{pm} = 1.0$ and $\varepsilon_{pm} = 3.0$ under the driving force $F = 0.5$. For both strong and weak attraction strengths, $\tau_1 \ll \tau$. For weak attraction strength $\varepsilon_{pm} = 1.0$, we find $\tau_3 \ll \tau_2$ and thus $\tau \approx \tau_2$.

strength. The value $\varepsilon_{pm} = 1.0$ corresponds to a weak interaction whereas $\varepsilon_{pm} = 3.0$ corresponds to the strong attraction limit. Here, $n_{trans} = 0$ before the first monomer exits the pore and $n_{trans} = N$ after the last monomer has threaded through the pore. As shown in Fig. 3, under the weak driving force $F = 0.5$, τ_1 is not sensitive to the attraction strength and $\tau_1 \ll \tau_2$. τ_2 for the strong attraction with $\varepsilon_{pm} = 3.0$ is roughly twice as that for the weak attraction with $\varepsilon_{pm} = 1.0$. However, τ_3 depends strongly on the attraction strength. For $\varepsilon_{pm} = 1.0$, $\tau_3 \ll \tau_2$ and is basically negligible for the pore length $L = 5$. For the strong attraction limit with $\varepsilon_{pm} = 3.0$, the situation is totally different with τ_3 more than an order of magnitude larger than τ_2 , completely dominating the total contribution to the translocation time. From Fig. 3, it can be seen that the number of translocated monomers oscillates around $n_{trans} \approx 122$, which corresponds to the beginning of the last stage of the translocation process, namely the emptying of the pore. This is due to the activated nature of the translocation process with a free energy difference of $\Delta\tilde{F} = L(\varepsilon_{pm} - F/2 - f(N))$ between the final and the initial state. The term $f(N)$ here accounts for the entropic driving force which should kick in at larger values of N , and eventually saturate for very long polymers. This leads to the long oscillation time of the last few monomers with repeated forward and backward motions. The final emptying of the pore corresponds to a rare crossing of the barrier.

To provide more microscopic details of the translocation process, we investigate the waiting time distribution for different chain lengths N in the strong attraction limit. The waiting time of monomer s is defined as the average time between the events that monomer s and monomer $s+1$ exit the pore. In our previous work [46, 47] for pure repulsive monomer-pore interactions, we found

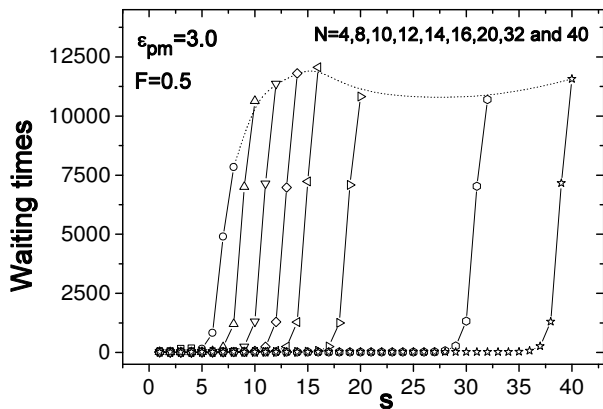


FIG. 4: Waiting time of different chain lengths for $\varepsilon_{pm} = 3.0$ and $F = 0.5$.

that the waiting time depends strongly on the monomer positions in the chain. For relatively short polymers, the monomers in the middle of the polymer need the longest time to exit the pore. Here, the waiting time of different chain lengths for $\varepsilon_{pm} = 3.0$ and $F = 0.5$ are shown in Fig. 4. It can be seen that it takes much longer time for last three monomers to exit the pore, which is completely different from that for pure repulsive monomer-pore interactions. This behavior correlates with the oscillation of the last monomers as shown in Fig. 3. Here we should mention that due to the entropic factor $f(N)$ in the barrier the waiting time for these last few monomers actually decreases in the range $N \approx 14 - 32$ before saturating and even increasing slightly with further increase of N .

Under zero and low driving forces, the translocation probability is very small in the sense that many translocation events, once started do not finish all the way. Instead, the polymer returns and exits to the cis side again. This means that the τ_1 process of filling the pore do not get completed and the real translocation process corresponding to τ_2 and τ_3 never even get started. We define an additional residence time τ_r as the weighted average of the translocation time for the completed events and the return time for the events that start and return via the cis side. The significance of this quantity is that it corresponds to the experimentally measured average blockage time of the polymer in the nanopore which does not distinguish return events from the completed translocated events. For zero or low driving force ($F < 0.5$), the residence time is almost completely dominated by return events. We have calculated the residence time τ_r for $\varepsilon_{pm} = 2.5$ and 3 in Fig. 5. As shown in Ref. 50, in the strong attraction case with $\varepsilon_{pm} = 3.0$, the N dependence of the residence time here is non-monotonic. This result of τ_r is in good agreement with experimental data of Krasilnikov *et al.* [67] where the residence time of a neutral PEG molecule in α -hemolysin pore was measured. Here, we further show that for $\varepsilon_{pm} = 2.5$, τ_r increases with increasing N . It indicates that the strong

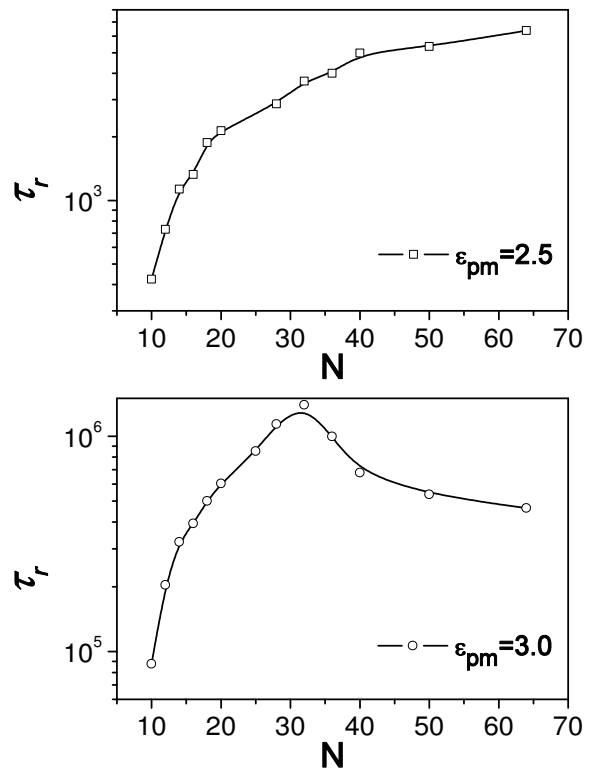


FIG. 5: Residence time τ_r as a function of the chain length for $\varepsilon_{pm} = 3.0$ and $\varepsilon_{pm} = 2.5$ under the driving force $F = 0$.

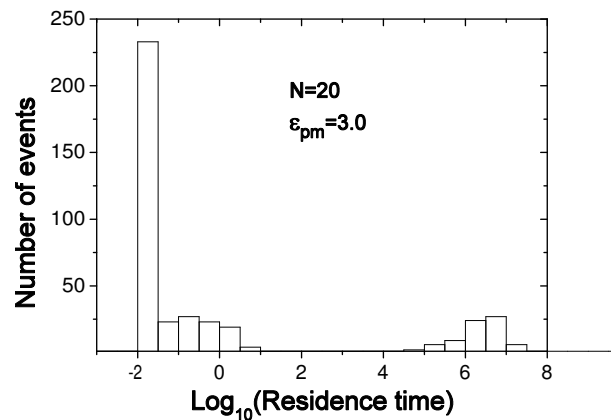


FIG. 6: Distribution of the residence time for $\varepsilon_{pm} = 3.0$ and $F = 0$. The chain length $N = 20$.

attraction plays an essential role in the observed non-monotonic behavior.

For $\varepsilon_{pm} = 3.0$, the distribution of τ_r is shown in Fig. 6. One obvious feature is the existence of two groups. The first group with shorter τ_r corresponds to the events where one end of the chain accesses the pore, and then quickly returns back. For the second group with longer τ_r , the residence time is still about 99.8% due to return events for $\varepsilon_{pm} = 3.0$. In the strong attraction limit, once the attractive force reaches its maximum when the pore is fully filled by monomers, it takes a very long time for

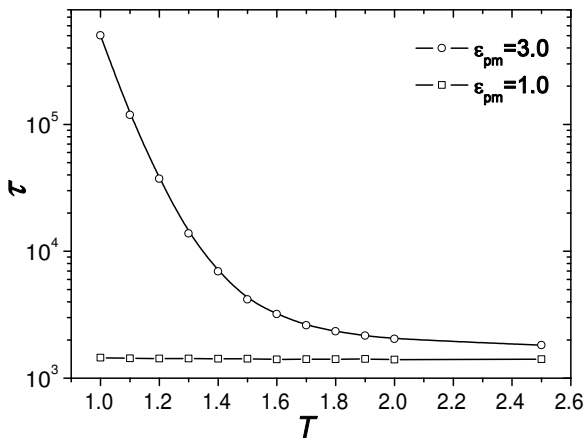


FIG. 7: Translocation time as a function of the temperature for both strong and weak attraction strengths ($\varepsilon_{pm} = 3.0$ and 1, respectively) under the driving force $F = 0.5$. The chain length $N = 128$.

the polymer to return back due to frequent backward and forward events.

B. Dependence of translocation time on various parameters

1. Translocation time as a function of temperature

Fig. 7 shows the translocation time τ as a function of the temperature for different attraction strengths. For the whole examined range of temperatures, τ decreases very slightly with increasing temperature for a weak attractive strength of $\varepsilon_{pm} = 1.0$. However, for the strong attractive strength $\varepsilon_{pm} = 3.0$, with increasing temperature τ first rapidly decreases and then approaches saturation at higher temperatures. At higher temperatures, the differences between translocation times for weak and strong attractive strengths become very small. This temperature dependence of translocation time is in good agreement with experiments [4].

2. Translocation time as a function of the driving force

In the weak attraction (*i.e.* non-activated) region, the overall τ is determined mainly by τ_2 and its dependence on the driving force scales as F^{-1} . This simple scaling behavior can be understood by considering the steady state of motion of the polymer through the nanopore. The average velocity is determined by balancing the frictional damping force (proportional to the velocity) with the external driving force. This leads to an average velocity proportional to the driving force F , and hence a translocation time $\tau \sim F^{-1}$. In Fig. 8 we show the dependence of the translocation time τ on the driving force. It can be seen that in the weak interaction limit

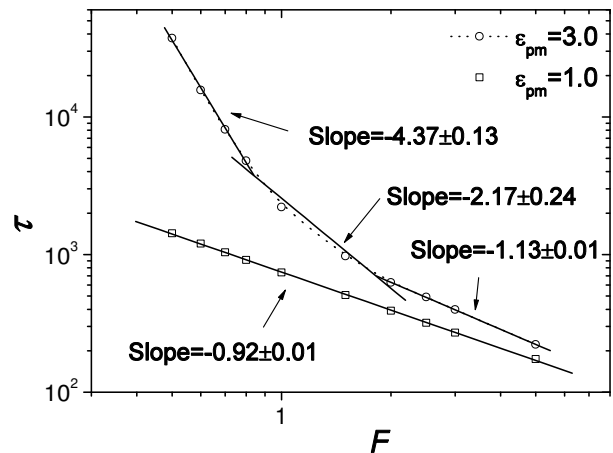


FIG. 8: Translocation time as a function of the driving forces for both strong and weak attraction strengths, $\varepsilon_{pm} = 3$ and 1. The chain length $N = 128$.

for $\varepsilon_{pm} = 1.0$ the data are very close to the linear scaling behavior $\tau \sim F^{-1}$ as predicted. For strong attractive interaction with $\varepsilon_{pm} = 4.0$, the situation is more complicated. For weak driving forces ($F \leq 2$), one is in the activated region where the inverse of the translocation time obeys an Arrhenius form. However, the driving force F affects both the activation barrier and the prefactor, leading to a complicated dependence of τ on the driving force that does not have a simple power law scaling form as seen in Fig. 8 for the $\varepsilon_{pm} = 3.0$ result. Insistence on fitting the data with a power law scaling form will lead to an effective scaling exponent that changes with the value of the driving force. Finally, beyond a critical force, the activation barrier disappears and one should obtain asymptotically the $\tau \sim F^{-1}$ behavior just as in the weak interaction case. This whole scenario is very similar to the sliding friction of an adsorbed layer under an external driving force [72].

The above theoretical considerations lead to a possible explanation of recent apparently conflicting experimental data. Polyuridylic acid (poly(U)) has a weak interaction with the pore, and it is not surprising that an inverse linear dependence of the translocation time on applied voltage was observed in experiments on the translocation of poly(U) [1]. However, Poly(dA) has much stronger interaction with the pore compared with poly(U). Thus it should be in the strong interaction activated region with a larger *effective* scaling exponent. Indeed, an inverse quadratic dependence of the translocation time on applied voltage had been experimentally observed for poly(dA) [5]. In view of our theoretical considerations, it would be desirable to have measurement over a larger range of the applied voltage to see the predicted change of effective scaling exponent.

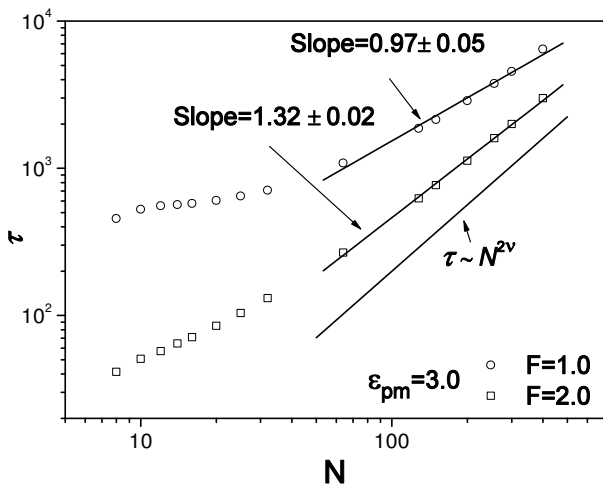


FIG. 9: Translocation time as a function of the chain length for $\varepsilon_{pm} = 3.0$ under $F = 1.0$ and $F = 2.0$, respectively.

3. Translocation time as a function of chain length

Previously, we have established that for pure repulsive polymer-pore interactions, the dependence of the translocation time on the length of the polymer scales as $\tau \sim N^{2\nu}$ for $N < 200$ and crosses over to a new scaling regime $\tau \sim N^{1+\nu}$ for larger values of N [46, 47, 49]. In the presence of weak interaction between the monomer and the pore, the qualitative dependence on the length of the polymer remains the same. For stronger attractive strength $\varepsilon_{pm} = 3.0$, the scaling exponent of τ with N for $64 \leq N \leq 400$ becomes strongly dependent on the driving force, with no indication of crossover behavior as shown in Fig. 9. We find $\tau \sim N^{1.32}$ for $F = 2.0$, which is close to $\tau \sim N^{2\nu}$ with the Flory exponent $\nu = 0.75$ in 2D [68, 69], and $\tau \sim N^{0.97}$ for $F = 1.0$. The novel dependence on the length of polymer is due to the change from the non-activated regime for weak attractive or pure repulsive interaction to an activated regime for strong attractive interaction.

Experimentally, a linear dependence $\tau \sim N$ was observed in experiments [1, 5] for polymer translocation through α -hemolysin channel, in contrast to the $\tau \sim N^{2\nu}$ scaling observed for polymer translocation through the solid-state nanopore [21]. This difference can be understood in light of our present results concerning the influence of the different polymer-pore interaction on the length dependence of the translocation time. For a synthetic pore, there is at most a very weak attractive interaction between the polymer and the pore and one expects the scaling behavior $\tau \sim N^{2\nu}$ to hold for $N \leq 200$. However, a stronger attractive interaction is expected to exist between the different bases and the α -hemolysin channel. For the models studied in this work, it changes the scaling behavior from $\tau \sim N^{2\nu}$ to $\tau \sim N$. This provides a possible explanation for the difference of the experimental observations in the different nanopores [1, 5, 21].

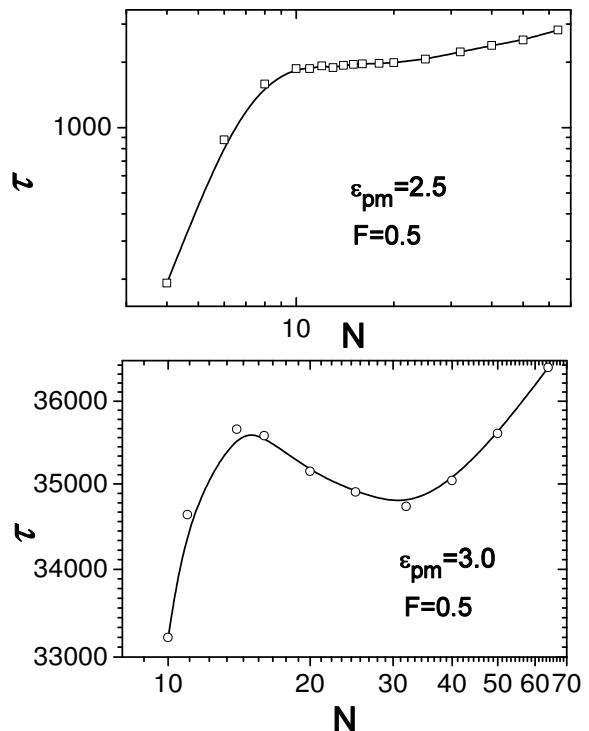


FIG. 10: Translocation time τ as a function of the chain length for $\varepsilon_{pm} = 3.0$ and $\varepsilon_{pm} = 2.5$ under the driving force $F = 0.5$.

Under a strong attractive force with $\varepsilon_{pm} = 3.0$ and a weak driving force $F = 0.5$, the translocation time τ has a qualitatively different dependence on N as compared with the pure repulsive or weak attractive pore interaction. Here we should mention that for $F = 0.5$ we cannot access $N > 128$ as the translocation time becomes too long to be feasible for numerical computation. As shown earlier in Ref. 50 and here in Fig. 10, the translocation time displays novel non-monotonic behavior with a rapid increase to a maximum at $N \sim 14$, followed by a decrease for $14 < N < 32$ and an increase again for $N > 32$. The eventual increase in the large N limit is due to the τ_2 contribution for longer chains. The observed non-monotonic behavior is also reflected qualitatively in the waiting time distribution as shown in Fig. 4. As shown in Fig. 10, with decreasing an attractive force to $\varepsilon_{pm} = 2.5$, this non-monotonic behavior vanishes.

To understand the microscopic origin, in Fig. 11 we show $\tau_1 + \tau_2$ as a function of the chain length for different attraction strengths under the driving force $F = 0.5$. For $32 \leq N \leq 200$, $\tau_1 + \tau_2 \sim N^{2\nu}$ is observed, irrespective of attraction strengths. This indicates that the novel non-monotonic behavior shown in Fig.10 in the strong interaction limit is again due to the pore-emptying process corresponding to τ_3 dominating the translocation time in strong interaction limit.

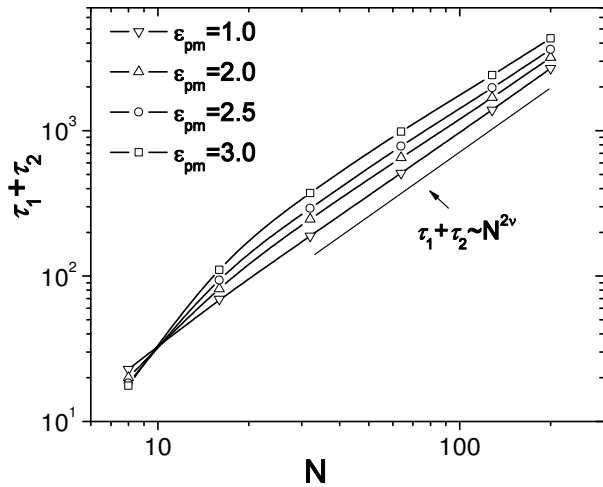


FIG. 11: $\tau_1 + \tau_2$ as a function of the chain length for different ϵ_{pm} under the driving force $F = 0.5$.

IV. CONCLUSIONS

In this work, we have studied the dependence of the translocation time on the temperature, attraction strength, driving force and the chain length. To analyze the influence of the attractive interaction in more detail, we have considered the three components of the

translocation time $\tau \approx \tau_1 + \tau_2 + \tau_3$, which were examined as a function of the attraction strength. Here τ_1 , τ_2 and τ_3 correspond to initial filling of the pore, transfer of polymer from the *cis* side to the *trans* side, and emptying of the pore, respectively. We find that $\tau_1 \ll \tau_2$ for both weak and strong attraction strengths, for N in the typical range used in the experiments. However, τ_3 is sensitive to the presence of an attractive interaction and changes from a value much less than τ_2 for weak interactions to the dominant contribution to the overall translocation time due to the rare activated event nature of the final emptying of the pore. This leads to a drastic change of the translocation dynamics and various scaling exponents as a function of the strength of the attractive monomer pore interactions. Our theoretical results are in good agreement with recent experimental data [4, 6, 67]. They also provide a possible explanation for the difference of the scaling behaviors with regard to the driving force and the length of polymers observed using different types of nanopores [1, 5, 21].

Acknowledgments

This work has been supported in part by The Academy of Finland through its Center of Excellence (COMP) and TransPoly Consortium grants.

-
- [1] J. J. Kasianowicz, E. Brandin, D. Branton and D. W. Deamer, *Proc. Natl. Acad. Sci. U.S.A.* **93**, 13770 (1996).
 [2] A. Meller, *J. Phys.: Condens. Matter* **15**, R581 (2003).
 [3] M. Akesson, D. Branton, J. J. Kasianowicz, E. Brandin, and D. W. Deamer, *Biophys. J.* **77**, 3227 (1999).
 [4] A. Meller, L. Nivon, E. Brandin, J. A. Golovchenko, and D. Branton, *Proc. Natl. Acad. Sci. U.S.A.* **97**, 1079 (2000).
 [5] A. Meller, L. Nivon, and D. Branton, *Phys. Rev. Lett.* **86**, 3435 (2001).
 [6] A. Meller and D. Branton, *Electrophoresis* **23**, 2583 (2002).
 [7] M. Wanunu and A. Meller, *Nano Lett.* **7**, 1580 (2007).
 [8] S. M. Iqbal, D. Akin, and R. Bashir, *Nat. Nanotech.* **2**, 243 (2007).
 [9] A. F. Sauer-Budge, J. A. Nyamwanda, D. K. Lubensky, and D. Branton, *Phys. Rev. Lett.* **90**, 238101 (2003).
 [10] J. Mathe, H. Visram, V. Viasnoff, Y. Rabin, and A. Meller, *Biophys. J.* **87**, 3205 (2004).
 [11] S. E. Henrickson, M. Misakian, B. Robertson, and J. J. Kasianowicz, *Phys. Rev. Lett.* **85**, 3057 (2000).
 [12] J. L. Li, D. Stein, C. McMullan, D. Branton, M. J. Aziz, and J. A. Golovchenko, *Nature (London)* **412**, 166 (2001).
 [13] J. L. Li, M. Gershow, D. Stein, E. Brandin, and J. A. Golovchenko, *Nat. Mater.* **2**, 611 (2003).
 [14] D. Fologea, J. Uplinger, B. Thomas, D. S. McNabb, and J. L. Li, *Nano Lett.* **5**, 1734 (2005).
 [15] U. F. Keyser, J. B. M. Koelman, S. van Dorp, D. Krapf, R. M. M. Smeets, S. G. Lemay, N. H. Dekker, and C. Dekker, *Nat. Phys.* **2**, 473 (2006).
 [16] U. F. Keyser, J. van der Does, C. Dekker, and N. H. Dekker, *Rev. Sci. Instr.*, **77**, 105105 (2006).
 [17] C. Dekker, *Nat. Nanotech.* **2**, 209 (2007).
 [18] E. H. Trepagnier, A. Radenovic, D. Sivak, P. Geissler, and J. Liphardt, *Nano Lett.* **7**, 2824 (2007).
 [19] A. J. Storm, J. H. Chen, X. S. Ling, H. W. Zandbergen, and C. Dekker, *Nat. Mater.* **2**, 537 (2003).
 [20] A. J. Storm, J. Chen, H. Zandbergen, and C. Dekker, *Phys. Rev. E* **71**, 051903 (2005).
 [21] A. J. Storm, C. Storm, J. Chen, H. Zandbergen, J. -F. Joanny and C. Dekker, *Nano Lett.* **5**, 1193 (2005).
 [22] S. M. Simon, C. S. Peskin, and G. F. Oster, *Proc. Natl. Acad. Sci. U.S.A.* **89**, 3770 (1992).
 [23] W. Sung and P. J. Park, *Phys. Rev. Lett.* **77**, 783 (1996).
 [24] P. J. Park and W. Sung, *J. Chem. Phys.* **108**, 3013 (1998).
 [25] E. A. diMarzio and A. L. Mandell, *J. Chem. Phys.* **107**, 5510 (1997).
 [26] M. Muthukumar, *J. Chem. Phys.* **111**, 10371 (1999).
 [27] M. Muthukumar, *J. Chem. Phys.* **118**, 5174 (2003).
 [28] C. Y. Kong and M. Muthukumar, *Electrophoresis* **23**, 2697 (2002); C. Y. Kong and M. Muthukumar, *J. Chem. Phys.* **120**, 3460 (2004); C. Y. Kong and M. Muthukumar, *J. Am. Chem. Soc.* **127**, 18252 (2005); M. Muthukumar and C. Y. Kong, *Proc. Natl. Acad. Sci. U.S.A.* **103**, 5273 (2006); C. Forrey and Muthukumar, *J. Chem. Phys.* **127**, 015102 (2007); C. T. A. Wong and M. Muthukumar,

- J. Chem. Phys.* **128**, 154903 (2008).
- [29] D. K. Lubensky and D. R. Nelson, *Biophys. J.* **77**, 1824 (1999).
- [30] Y. Kafri, D. K. Lubensky, and D. R. Nelson, *Biophys. J.* **86**, 3373 (2004).
- [31] E. Slonkina and A. B. Kolomeisky, *J. Chem. Phys.* **118**, 7112 (2003); S. Kotsev and A. B. Kolomeisky, *J. Chem. Phys.* **125**, 084906 (2006); A. Mohan, A. B. Kolomeisky and M. Pasquali, *J. Chem. Phys.* **128**, 125104 (2008).
- [32] S. Matysiak, A. Montesi, M. Pasquali, A. B. Kolomeisky, and C. Clementi, *Phys. Rev. Lett.* **96**, 118103 (2006).
- [33] T. Ambjornsson, S. P. Apell, Z. Konkoli, E. A. DiMarzio, and J. J. Kasianowicz, *J. Chem. Phys.* **117**, 4063 (2002).
- [34] R. Metzler and J. Klafter, *Biophys. J.* **85**, 2776 (2003).
- [35] T. Ambjornsson and R. Metzler, *Phys. Biol.* **1**, 19 (2004).
- [36] T. Ambjornsson, M. A. Lomholt, and R. Metzler, *J. Phys.: Condens. Matter* **17**, S3945 (2005).
- [37] A. Baumgartner and J. Skolnick, *Phys. Rev. Lett.* **74**, 2142 (1995).
- [38] J. Chuang, Y. Kantor and M. Kardar, *Phys. Rev. E* **65**, 011802 (2002).
- [39] Y. Kantor and M. Kardar, *Phys. Rev. E* **69**, 021806 (2004).
- [40] J. K. Wolterink, G. T. Barkema, and D. Panja, *Phys. Rev. Lett.* **96**, 208301 (2006); D. Panja, G. T. Barkema, and R. C. Ball, *J. Phys.: Condens. Matter* **19**, 432202 (2007); D. Panja and G. T. Barkema, *Biophys. J.* **94**, 1630 (2008).
- [41] D. Panja, G. T. Barkema, and R. C. Ball, *J. Phys.: Condens. Matter* **20**, 075101 (2008); H. Vocks, D. Panja, G. T. Barkema, and R. C. Ball, *J. Phys.: Condens. Matter* **20**, 095224 (2008).
- [42] J. L. A. Dubbeldam, A. Milchev, V.G. Rostiashvili, and T.A. Vilgis, *Phys. Rev. E* **76**, 010801(R) (2007).
- [43] J. L. A. Dubbeldam, A. Milchev, V.G. Rostiashvili, and T.A. Vilgis, *Europhys. Lett.* **79**, 18002 (2007).
- [44] A. Milchev, K. Binder, and A. Bhattacharya, *J. Chem. Phys.* **121**, 6042 (2004).
- [45] K. F. Luo, T. Ala-Nissila, and S. C. Ying, *J. Chem. Phys.* **124**, 034714 (2006).
- [46] K. F. Luo, I. Huopaniemi, T. Ala-Nissila, and S. C. Ying, *J. Chem. Phys.* **124**, 114704 (2006).
- [47] I. Huopaniemi, K. F. Luo, T. Ala-Nissila, and S. C. Ying, *J. Chem. Phys.* **125**, 124901 (2006).
- [48] I. Huopaniemi, K. F. Luo, T. Ala-Nissila, and S. C. Ying, *Phys. Rev. E* **75**, 061912 (2007).
- [49] K. F. Luo, T. Ala-Nissila, S. C. Ying, and A. Bhattacharya, *J. Chem. Phys.* **126**, 145101 (2007).
- [50] K. F. Luo, T. Ala-Nissila, S. C. Ying, and A. Bhattacharya, *Phys. Rev. Lett.* **99**, 148102 (2007).
- [51] K. F. Luo, T. Ala-Nissila, S. C. Ying, and A. Bhattacharya, *Phys. Rev. Lett.* **100**, 058101 (2008).
- [52] K. F. Luo, T. Ala-Nissila, S. C. Ying, and A. Bhattacharya, to be published.
- [53] K. F. Luo, T. Ala-Nissila, S. C. Ying, P. Pomorski and M. Kattunen, arXiv:0709.4615.
- [54] S. Guillouezic and G. W. Slater, *Phys. Lett. A* **359**, 261 (2006); M. G. Gauthier and G. W. Slater, *Eur. Phys. J. E* **25**, 17 (2008); M. G. Gauthier and G. W. Slater, *J. Chem. Phys.* **128**, 065103 (2008).
- [55] S.-S. Chern, A. E. Cardenas, and R. D. Coalson, *J. Chem. Phys.* **115**, 7772 (2001).
- [56] H. C. Loebel, R. Randel, S. P. Goodwin, and C. C. Matthai, *Phys. Rev. E* **67**, 041913 (2003).
- [57] R. Randel, H. C. Loebel, and C. C. Matthai, *Macromol. Theory Simul.* **13**, 387 (2004).
- [58] Y. Lansac, P. K. Maiti, and M. A. Glaser, *Polymer* **45**, 3099 (2004).
- [59] Z. Farkas, I. Derenyi, and T. Vicsek, *J. Phys.: Condens. Matter* **15**, S1767 (2003).
- [60] P. Tian and G. D. Smith, *J. Chem. Phys.* **119**, 11475 (2003).
- [61] Y. D. He, H. J. Qian, Z. Y. Lu, and Z. S. Li, *Polymer* **48**, 3601 (2007); Y. C. Chen, C. Wang, and M. Luo, *J. Chem. Phys.* **127**, 044904 (2007); Y. J. Xie, H. Y. Yang, H. T. Yu, Q. W. Shi, X. P. Wang, and J. Chen, *J. Chem. Phys.* **124**, 174906 (2006).
- [62] D. Wei, W. Yang, X. Jin, and Q. Liao, *J. Chem. Phys.* **126**, 204901 (2007).
- [63] M. B. Luo, *Polymer* **48**, 7679 (2007).
- [64] R. Zandi, D. Reguera, J. Rudnick, and W. M. Gelbart, *Proc. Natl. Acad. Sci. U.S.A.* **100**, 8649 (2003).
- [65] S. Tsuchiya and A. Matsuyama, *Phys. Rev. E* **76**, 011801 (2007).
- [66] A. Bhattacharya *et al.*, unpublished (2008).
- [67] O. V. Krasilnikov, C. G. Rodrigues, and S. M. Bezrukov, *Phys. Rev. Lett.* **97**, 018301 (2006).
- [68] P. G. de Gennes, *Scaling Concepts in Polymer Physics* (Cornell University Press, Ithaca, NY, 1979).
- [69] M. Doi, and S. F. Edwards, *The Theory of Polymer Dynamics* (Clarendon, Oxford, 1986).
- [70] M.P. Allen, D.J. Tildesley, *Computer Simulation of Liquids* (Oxford University Press, 1987).
- [71] D. L. Ermak and H. Buckholz, *J. Comput. Phys.* **35**, 169 (1980).
- [72] E. Granato and S. C. Ying, *Phys. Rev. Lett.* **85**, 5368 (2000).